

# STIFFNESS AND FRACTURE OF SHEAR LOADED LAMINATES WITH UNIDIRECTIONAL AND BIAXIAL FIBRE ORIENTATION INVESTIGATED WITH A PICTURE FRAME TEST

V. Trappe<sup>a\*</sup>, R. Basan<sup>b</sup>, F. Grasse<sup>c</sup>

<sup>a</sup>Federal Institute for Materials Research and Testing, Unter den Eichen 87, 12205 Berlin

<sup>b</sup>Siemens AG, Huttenstraße 12, 10553 Berlin

<sup>c</sup>Grasse Zur Ingenieurgesellschaft mbH, Hohentwielsteig 6a, 14163 Berlin

\*volker.trappe@bam.de

**Keywords:** picture frame test, fibre reinforced plastics (FRP), shear strength and stiffness, in-situ effect

## Abstract

*Fibre Reinforced Plastics (e.g. CFRP, GFRP) characteristically show nonlinear stress-strain behaviour due to intralaminar shear loading. The determination of the in-plane shear stiffness and strength for this class of material is difficult and common test standards and methods of analysis are partially inaccurate. The identification of the in-plane shear properties was made with an especial designed “picture frame test device” which enables shear loading up to 950N/mm. Therefore the strength limit can be reached at specimens with adequate thickness and a high safety factor against buckling. Due to the chosen design the maximum of the shear loading and the final failure occur in the centre of the specimen. The experiments match with the numerical analysis.*

## 1. Introduction

The classical laminate theory and the layer-wise strength analysis [1, 2] are state of the art for the dimensioning of a high performance light weight structure made of carbon or glass fibre reinforced plastics (CFRP, GFRP). The authors are convinced and there are certain findings [3, 4] that a high inter fibre failure (IFF) loading causes especially a shortened fatigue life of FRPs. Hence, all material parameters stiffness and strength for the regarded composite must be well known for a proper in-service design.

The experimental determination of strength and stiffness of a single unidirectional layer in and perpendicular to the fibre direction can be performed simply with an unidirectional tension or compression test [5, 6] with sufficient precision. Meanwhile it is not so easy to determine experimentally strength and stiffness due to pure intralaminar shear. There are several standards available to determine the shear modulus  $G_{\perp\parallel}$  and the shear strength  $R_{\perp\parallel}$  e.g. according to Iosipescu [7, 8] or the rail shear test [9]. Both methods have the disadvantage of an inhomogeneous parabolic shear loading due to the transverse force loading and the v-notch can cause further problems. Additionally, the non-linear stress strain behaviour of FRP due to intralaminar shear loading causes an unjustified fibre orientation and hence a combined shear-transverse inter fibre failure. The tensile test of  $\pm 45^\circ$ -laminates [10, 11] is very simple to

perform and gives sufficient results for the shear stiffness  $G_{\perp\parallel}$ . However, the determined in-plane shear strength  $R_{\perp\parallel}$  is inaccurate due to the in-situ effect of the adjacent layers [12, 13].

Experimentally pure in-plane shear loading can be realized with tube specimens [14, 15] or a shear frame test set-up, better known as “picture frame test” [16]. The tube specimen has the further advantage to be loaded biaxial in tension torsion and hence the complete fracture surface of an UD-layer can be determined. However the disadvantage is the high effort and cost to manufacture UD-tube specimens in filament winding technique and consequently not all textile preforms could be formed in tube specimens with sufficient quality. In a shear frame set-up plane specimens and hence a wide variety of preforms can be tested simply. This “picture frame” technique is successfully used for draping predictions of woven textiles [17, 18] at comparably low shear loads. For measuring the in-plane shear strength and stiffness of continuous fibre reinforced composites there is a standard given [16], however, the findings were carried out as “complicated” [19].

In a research project [20] an especially designed shear frame apparatus was developed. The dimensioning against buckling and the clamping of the specimens were addressed. Additionally, the shear strain field was numerically analyzed and experimentally evaluated. With this technique the in-plane shear modulus  $G_{\perp\parallel}$  ( $\gamma$ ) was determined. Subsequently the inter fibre loading of a  $\pm 45^\circ$ -laminates in a tensile test was analysed stepwise.

## 2. Experimental

### 2.1 Design and numerical analysis of the shear frame apparatus

In the first step the specimens have to be dimensioned against buckling to enable a geometric linear measurement of the in-plane shear modulus  $G_{\perp\parallel}$  and the shear strength  $R_{\perp\parallel}$ . Therefore the buckling shear stress  $\tau_{\perp\parallel}$  has to be higher than the shear strength of the specimen. According to [21] the critical buckling stress is given as:

$$\tau_{\perp\parallel, krit} = k_{\tau_{\perp\parallel}} \left(\frac{\pi}{l}\right)^2 \sqrt[4]{D_{11}D_{22}^3} \quad (1)$$

The bending stiffness  $D_{11}$  and  $D_{22}$  ( $x_1$ - and  $x_2$ -direction) is given according to [1] with the material parameters given in table 1 [20]. The buckling coefficient  $k_{\tau_{\perp\parallel}}$  of an orthotropic material depends on the support, the geometry, the bending stiffness and the secant shear modulus  $G_{\perp\parallel}$ , which decreases with the shear deformation (s. figure 5). For a quadratic FRP-plate and fixed-end support the coefficients are given in table 2.

material data FRP-specimens			material data shear frame apparatus		
quantity	GFRP	CFRP	quantity	steel	aluminium
$E_1$	32,380	97,940	E	210,000	70,000
$E_2 = E_3$	8,990	6,730	$\nu$	0.300	0.330
$G_{12} = G_{13}$	2,830	2,860			
$G_{23}$	3,211	2,404			
$\nu_{21} = \nu_{31}$	0.297	0.345			
$\nu_{23}$	0.400	0.400			

E and G in MPa,  $\nu$  dimensionless,  $E_1 = E_{\parallel}$ ,  $E_2 = E_{\perp}$ ,  $G_{12} = G_{\perp\parallel}$

**Table 1:** Material data for the analytical buckling examination and the numerical Finite Element Analysis [20].

	CFRP 0°	CFRP 0°/90°	GFRP 0°	GFRP 0°/90°
$k_{\tau\perp\parallel}(G_{\perp\parallel} = 2900 \text{ MPa})$	7.0	7.5	8.7	9.3
$k_{\tau\perp\parallel}(G_{\perp\parallel} = 500 \text{ MPa})$	6.1	6.8	7.2	7.8

**Table 2:** Buckling coefficients for different laminates respecting the support, the laminate lay-up and the decrease of in-plane shear modulus due to high shear deformation [20].

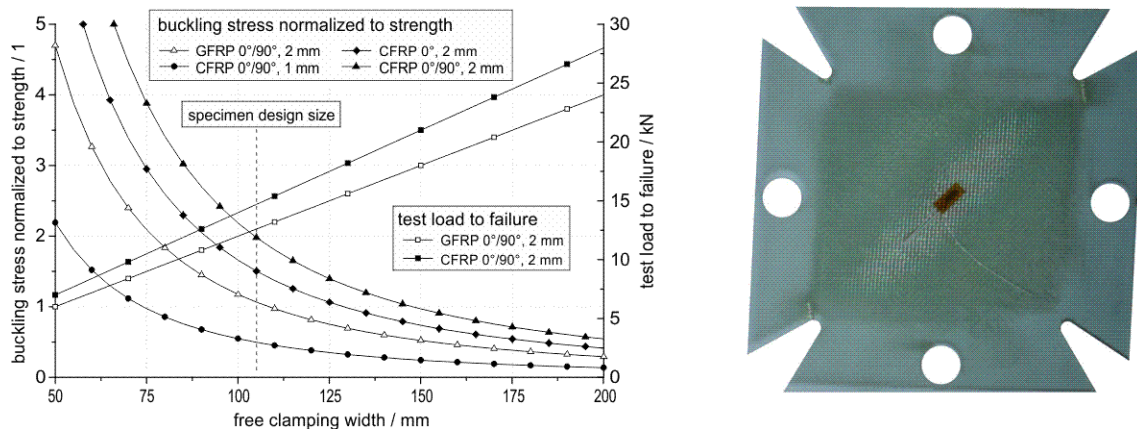


**Figure 1:** left – buckling stress and test load for CFRP and GFRP specimens of different size, laminate lay-up and thickness, right – 2mm GFRP specimen which failed due to buckling [20].

With these data and a reduced shear modulus of 500MPa an analytical linear buckling analysis was done for four different FRP laminates and a specimen width between the clamping of 50 to 200mm. The shear strength was estimated with 60MPa for GFRP and 70MPa for CFRP. The result is shown in figure 1- left. The free specimen design size was taken with 105mm which is a compromise to have enough space for the hinges, and sufficient clamping length on the one hand and thin specimens and low test forces on the other hand. The analysis shows that a 0°-laminate has a lower buckling stress than a 0°/90°-laminate. Additionally, there is no safety factor in the calculation. A test was done with a 2mm 0°/90°-laminate which is a little above 1 of the ratio of critical buckling stress to the laminate in-plane shear strength. The result was a failure due to buckling (s. figure 1 – right). Hence, at least a factor of 2 should be taken for the design, to take in account geometric inaccuracies of the specimens. This results in test loads of at least 15kN up to 25kN.

To enable the test of thick laminates the shear frame apparatus (s. figure 4 – left) was designed for a maximum test load of 100kN, hence, a maximum shear flow of about 950N/mm was achieved. The shear specimen is positioned between two shear frames with each 4 hinges. To overcome the disadvantage of an inconvenient mounting of the specimens and to ensure no slipping due to the transversal contraction of the FRP, the clamping forces are applied by four hydraulic cylinders with each 120kN maximum force. Hence, a simple handling was reached. However, due to the considerable size of the hinges and the single load application each side, a complete FEM analysis of the shear frame was done by the FE-program ANSYS. The details are given in [21]. The precise geometry of the specimens is shown in figure 3. From this follows a mean compression stress on the specimen in the clamping of 33MPa. The numerical result achieved from the FE-analysis shows (s. figure 2 - left) a peak value of 2.3 times of the mean value due to the flexibility of the frame. This is far below the transverse compression strength of the tested FRPs ( $R_{\perp} > 100\text{MPa}$ ). The numerical analysis of the shear strain field (s. figure 2 – middle and right) gives a peek value in the middle of the specimen of about 1,08 times of the mean shear stress derived from  $F_{\text{shear}}/(t \cdot l)$ , with the specimen thickness  $t$  and the specimen width  $l$  according to figure 3. This result is

promising because having the max stress in the centre of the specimens no edge effects will distort the failure mechanism.

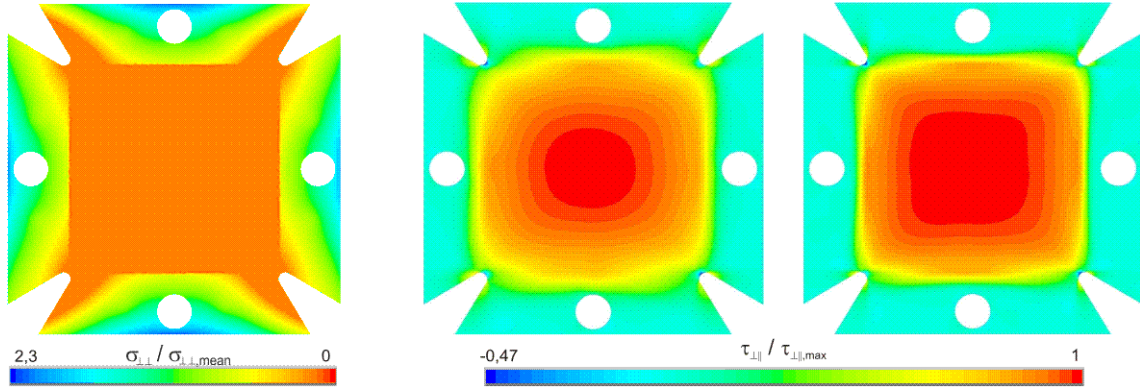


**Figure 2:** left – distribution of compression stress normalized to the mean value, middle – distribution of the in-plane shear stress normalized to the maximum value for GFRP, right – distribution for CFRP [20].

### 2.2 Shear tests 0°- and 0°/90°-laminates

According to figure 3-left the shear deformation  $\gamma$  is given as:

$$\gamma + 2\alpha = \frac{\pi}{2} \quad (2)$$

$\alpha$  can be replaced due to trigonometric relations (s. figure 3-left) and eq. 2 can be converted with the strain  $\epsilon$  to:

$$\gamma = \frac{\pi}{2} - 2\arccos\left(\frac{1+\epsilon}{\sqrt{2}}\right) \quad (3)$$

For small shear deformations the eq. 3 can be simplified [21] and the shear strain is given as:

$$\gamma \approx 2\epsilon \quad (4)$$

Additionally, the mean shear deformation can be defined with the displacement  $u$  and the width  $l$  to:

$$\bar{\gamma} = \arcsin\frac{u}{l} \quad (5)$$

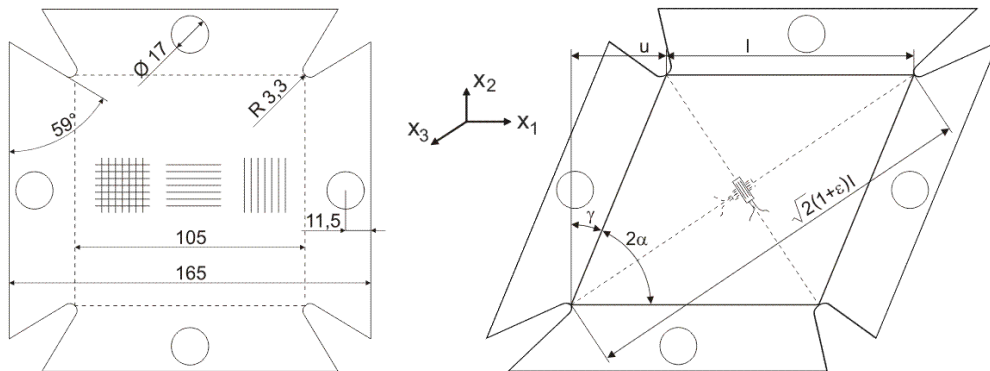


**Figure 3:** left – geometry of the shear specimen, right – definitions to calculate the shear strain [20].

Hence, the shear strain can be measured simply by strain gauges on the shear specimens or by the tensile displacement indicated by the sensor of the tensile testing machine. As figured out

by the FEM analysis the shear stress and hence the measured shear strain is about 8% higher as the mean value. This was evaluated for the GFRP specimens with additional strain gauges in the edges (s. figure 4 – middle). The measurements were in good accordance with the numerical analysis. Hence, the actual measured shear strain in the middle of the specimens in  $\pm 45^\circ$ -direction is too high compared to the mean value of shear stress indicated by the load cell of the tensile testing machine. This has to be considered in the experimental determination of the shear modulus  $G_{\perp\parallel}$  and the shear strength  $R_{\perp\parallel}$ .

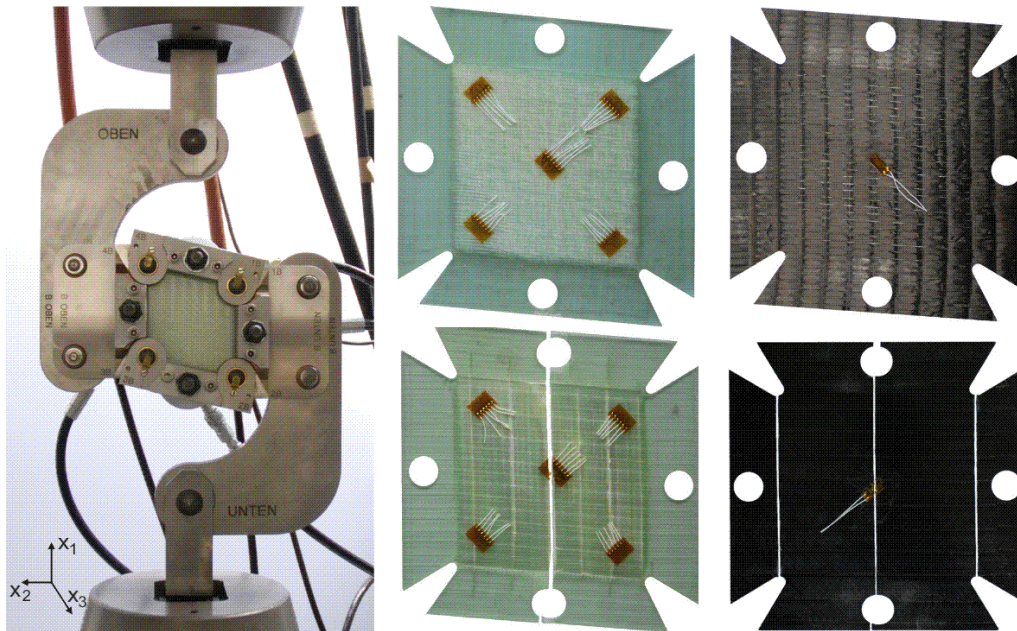


**Figure 4:** left – shear frame apparatus gripped in the tensile testing machine, middle and right – GFRP and CFRP shear specimens after testing (above –  $0^\circ/90^\circ$ -laminates, below –  $0^\circ$ -laminates)

GFRP and CFRP shear specimens were investigated with  $0^\circ$ - and  $0^\circ/90^\circ$ -fibre orientation made of non-crimp fabric (NCF). The failure behaviour of the  $0^\circ$ -laminates start with a sudden crack in the centre of the specimen which immediately travels over the whole width oriented parallel to the fibre direction. Successive cracks occur at higher shear strain at decreased load beside and parallel to the centre crack (s. Figure 4 – middle and right bottom). In the stress-strain diagram (s. figure 5) the stepwise decrease of strength with each crack can be observed. As in-plane shear strength was taken the stress value of the first inter-fibre failure.

In contrast the  $0^\circ/90^\circ$ -laminates show a high plasticity and no failure of the specimens was observed till the maximum possible shear deformation ( $\gamma \approx 25\%$ ) of the shear frame was reached (s. figure 4 – middle and right above). As in-plane shear strength was defined the point when the tangential modulus drops below 2% of the initial value, what means that there is no significant increase of shear stress anymore. Additionally, a  $0^\circ/90^\circ$ -CFRP made of a linen style fabric was tested and shows a quite similar strength and stiffness as the cross-ply laminate.

quantity	dimension	GFRP	CFRP
$R_{\perp}^{(+)}$	MPa	23.0	36.4
$R_{\perp}^{(-)}$	MPa	107.5	108.6
$R_{\perp\parallel}$	MPa	49.2	42.5

**Table 3:** IFF strength mean values experimentally derived according to [5, 6] and the shear frame tests for UD-laminates made from NCF (Cramer Style AUW) and MOMENTIVE L285 / H287 Epoxy-Matrix.



For both type of laminates the secant modulus  $G_{\perp\parallel}$  was derived from the sampling points at  $\gamma' = 0.001$  and  $\gamma'' = 0.005$  as quite similar defined in [10]. For GFRP a continuous stress whitening was observed due to micro-cracking (s. figure 5 – middle). In contrast, the  $0^\circ$ -laminate shows separated inter-fibre cracks. Additionally the in-plane shear strength of the cross ply laminates is about 15% higher for GFRP and more than 30% higher for CFRP as the UD-laminates (s. figure 5 and table 3). However, due to the classical laminate theory the results should be the same. Hence, the adjacent layers cause an in-situ effect which changes the fracture behaviour and increases the in-plane shear strength.

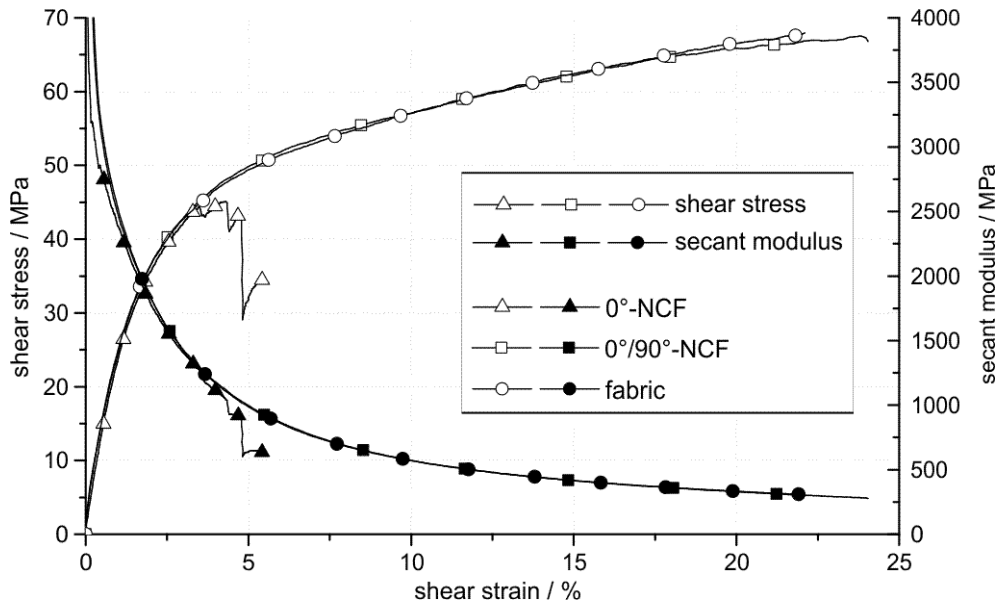


**Figure 5:** shear stress and secant modules vs. shear strain for  $0^\circ$ - and  $0^\circ/90^\circ$ -CFRP-laminates. Additionally, a  $0^\circ/90^\circ$ -CFRP made of a linen style fabric was tested [20].

### 2.3 $\pm 45^\circ$ -tension test method compared to shear frame test method

Due to its simplicity the  $\pm 45^\circ$ -tension test [10, 11] is favoured to determine the in-plane shear stiffness  $G_{\perp\parallel}$  and strength  $\tau_{\perp\parallel}$ . Perpendicular strain gauges were bonded on the tensile specimen in x- and y-direction and the shear strain is given as:

$$\gamma_{\perp\parallel} = \epsilon_x - \epsilon_y \quad (6)$$

The shear stiffness subsequently is defined with  $\sigma_x$  derived from the tensile load to:

$$G_{\perp\parallel} = \frac{\sigma_x}{2(\epsilon_x - \epsilon_y)} = \frac{\tau_{\perp\parallel}}{\gamma_{\perp\parallel}} \quad (7)$$

The shear strength is defined as the half of the maximum tensile stress at breakage or as  $0.5 \cdot \sigma_{x,5\%}$  at the sampling point at  $\gamma_{\perp\parallel} = 0.05$ . With the experimentally determined decreasing shear modules (s. figure 5) and the knowledge of the fibre rotation derived from

$$\omega = \arctan \frac{1 + \epsilon_x}{1 + \epsilon_y} - \frac{\pi}{4} \quad (8)$$

a layer-wise strength analysis could be done stepwise for the  $\pm 45^\circ$ -tension test. All other elastic quantities were considered as constant (according to table 1). The result is shown in figure 6, where the inter-fibre loading is opposed to the tensile test and 5 characteristic load

steps (s. table 4) were illustrated. In summary it appears that the in-plane shear modulus gained from  $\pm 45^\circ$ -tension test is quite similar to the shear frame experiment. However the inter fibre failure mechanism in those tests is quite different. The assumption of a fixed ratio of inter-fibre-transverse to -shear loading is wrong for the  $\pm 45^\circ$ -tension test and neither the stress at 5% strain nor the maximum stress match sufficient with the in-plane shear strength gained from the shear frame method.

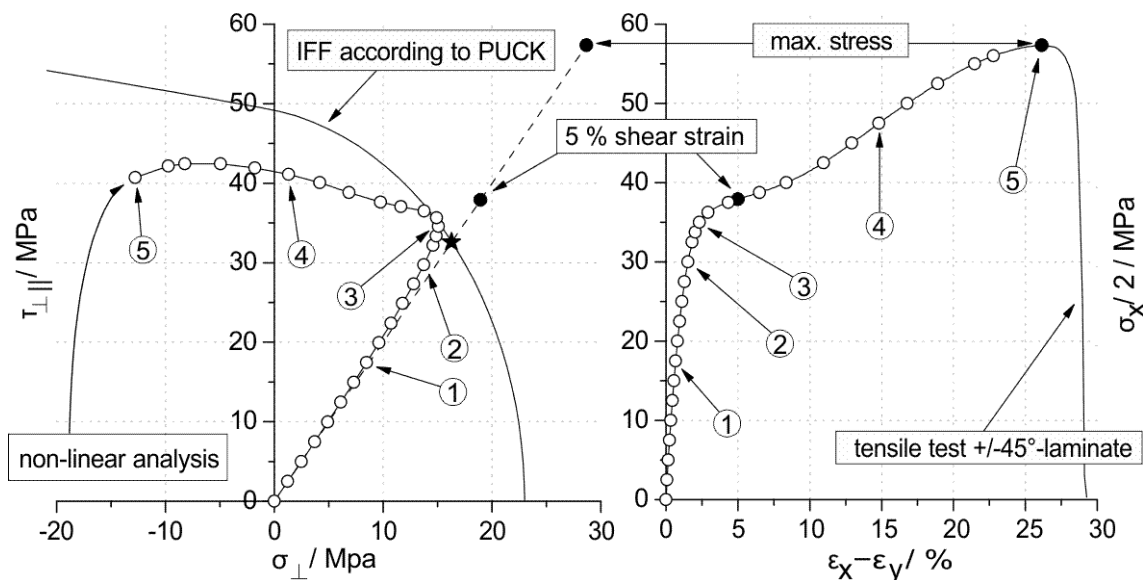


**Figure 6:** left - Inter fibre failure limit according to PUCK (calculated with the values of table 3) and layer-wise strength analysis of the  $\pm 45^\circ$ -tension test, right -  $\pm 45^\circ$ -tension test (the half tensile stress plotted vs. the shear strain [10]). In both diagrams corresponding load steps are marked [20].

load step	$\frac{\sigma_x}{2} / \text{MPa}$	$\omega / ^\circ$	$\sigma_{\parallel} / \text{MPa}$	$\sigma_{\perp} / \text{MPa}$	$\tau_{\perp\parallel} / \text{MPa}$	$G_{\perp\parallel} / \text{MPa}$
1	17.50	0.19	26.5	8.5	17.4	2,740
2	30.00	0.44	44.6	13.7	29.8	2,295
3	36.25	0.83	57.6	14.9	35.6	2,025
4	47.50	4.25	93.7	1.3	41.1	1,710
5	57.30	7.43	127.4	-12.8	40.7	1,625

**Table 4:** Stress state and fibre rotation at different load steps corresponding to figure 6 [20].

### 3. Conclusions

An especially designed “picture frame test” apparatus was developed for the convenient and precise determination of the in-plane shear strength and stiffness of FRPs. A maximum shear flow of about 950N/mm was realized and enables to test a wide variety of composite materials. A FEM-analysis of the complete apparatus was done and the calculated shear strain field was experimentally evaluated. Additionally a specification [22] was written according to common standards. Promising results were gained for  $0^\circ$ - and  $0^\circ/90^\circ$ -laminates made of NCF. In particular the influence of the adjacent layers on the shear strength was shown. The shear frame technique overcomes the impreciseness of several other methods. Exemplarily the  $\pm 45^\circ$ -tension test method was evaluated with the findings of the shear frame experiments and the differences in the inter fibre failure behaviour were carved out. Finally the shear frame apparatus was refined for commercial use and production [23].

## References

- [1] VDI 2014, "Development of FRP components (fibre-reinforced plastics) – Part 3 Analysis", Verein Deutscher Ingenieure (2006)
- [2] Puck, A., Schürmann, H.: "Failure analysis of FRP laminates by means of physically based phenomenological models. Part A"; Composites Science and Technology (58) 7, pp. 1045–1067, (1998)
- [3] Trappe, V., Harbich, K.-W., Ernst, H.: „Intralaminar fatigue behaviour of carbon fibre reinforced plastics“; Int. Journal of Fatigue 28, pp. 1187-1196, (2006)
- [4] Trappe; V. Ortwein, H.-P., Hickmann, S.: "Infinite life of CFRP evaluated nondestructively with X-ray-refraction topography", 19th International Conference on Composite Materials (Proceedings) ISBN:9781629931999, (2013)
- [5] DIN EN ISO 527-4, "Plastics - Determination of tensile properties – Part 4: Test conditions for isotropic and orthotropic fibre reinforced plastic composites", Deutsches Institut für Normung (1997)
- [6] DIN EN ISO 14126, "Fibre reinforced plastic composites - Determination of compressive properties in the in-plane direction", Deutsches Institut für Normung (1999)
- [7] Iosipescu, N.: "New Accurate Procedure for Single Shear Testing of Metals", Int. Journal of Materials (2) 3, p. 537–566, (1967)
- [8] ASTM D5379 / D5379M – 05, "Standard Test Method for Shear Properties of Composite Materials by the V-Notched Beam Method", American Society for Testing and Materials, (2005)
- [9] ASTM D7078 / D7078M - 05, "Test Method for Shear Properties of Composite Materials by V-Notched Rail Shear Method", American Society for Testing and Materials, (2005)
- [10] DIN EN ISO 14129, "Fibre-reinforced plastic composites –determination of the in-plane shear modulus and strength by the  $\pm 45^\circ$  tension test method, Deutsches Institut für Normung (1998)
- [11] ASTM D3518/D3518M – 94, "Test Method for In-Plane Shear Response of Polymer Matrix Composite Materials by Tensile Test of a  $\pm 45^\circ$  Laminate", American Society for Testing and Materials, (2007)
- [12] Trappe, V., Hickmann, S., Sturm, H.: „Bestimmung des Zwischenfaserbruchversagens in textilverstärktem Glasfaserkunststoff mittels der Röntgenrefractionstopografie“, MP Materials Testing (50) 10, pp. 615- 622, Hanser (2008)
- [13] Camanho, P., Davila, C.G., Pinho, S.T., Iannucci, L., Robinson, P.: "Prediction of in situ strengths and matrix cracking in composites under transverse tension and in-plane shear", Composites Part A 37, pp. 165-176, (2006)
- [14] Puck A, Schürmann H.: "Die Zug/Druck-Torsionsprüfung an rohrförmigen Probekörpern", Kunststoffe (72) 9, 554–561, (1982)
- [15] ASTM D5448 / D5448M, "Test Method for Inplane Shear Properties of Hoop Wound Polymer Matrix Composite Cylinders", American Society for Testing and Materials
- [16] DIN 53399-2, „Schubversuch an ebenen Probekörpern“, Deutsches Institut für Normung (1982)
- [17] Lebrun, G., Bureau, M., Denault, J.: "Evaluation of bias-extension and picture-frame test methods for the measurement of intraply shear properties of PP/glass commingled fabrics “, Composite Structures 61, pp.341–352, (2003)
- [18] Lomov, S.V., Willems, A., Verpoest, I., Zhu, Y., Barburski, M., Stoilova, T.: "Picture Frame Test of Woven Composite Reinforcements with a Full-Field Strain Registration, Textile Research Journal Vol 76 (3), pp. 243–252, (2006)
- [19] Chatterjee, S., Adams, D., Oplinger, D.W.: "Test Methods for Composites a Status Report – Volume III. Shear Test Methods", DOT/FAA/CT-93/17, III, 1993
- [20] Basan, R.: „Untersuchung der intralaminaren Schubeigenschaften von Faserverbundwerkstoffen mit Epoxidharzmatrix unter Berücksichtigung nichtlinearer Effekte“, BAM-Dissertationsreihe (Band 74), Berlin, 2011
- [21] Wiedemann, J.: „Leichtbau – Elemente und Konstruktion“, 3. Auflage, Springer-Verlag, Berlin-Heidelberg-New York, ISBN978-3-540-33656-3, (2007)
- [22] DIN SPEC 4885, "Fibre-reinforced plastic composites – Shear test method using a shear frame for the determination of the in-plane shear stress/shear strain response and shear modulus, Deutsches Institut für Normung (2014)
- [23] <http://grassezur.de/en/>